Journal of Experimental Botany, Vol. 59, No. 8, pp. 2147–2160, 2008
doi:10.1093/jxb/ern082
This paper is available online free of all access charges (see http://jxb.oxfordjournals.org/open_access.html for further details)

Journal of Experimental Botany
www.jxb.oxfordjournals.org

RESEARCH PAPER

Alteration in the chloroplastic metabolism leads to ROS accumulation in pea plants in response to plum pox virus

Pedro Díaz-Vivancos[1], María José Clemente-Moreno[1], Manuel Rubio[1], Enrique Olmos[2], Juan Antonio García[3], Pedro Martínez-Gómez[1] and José Antonio Hernández[1,*]

[1] *Department of Plant Breeding CEBAS-CSIC, PO Box 164, E-30100 Espinardo-Murcia, Spain*

[2] *Department of Biology of Stress and Plant Pathology CEBAS-CSIC. PO Box 164, E-30100 Espinardo-Murcia, Spain*

[3] *Department of Plant Molecular Genetics CNB-CSIC, E-28049 Madrid, Spain*

Received 11 December 2007; Revised 21 February 2008; Accepted 25 February 2008

Abstract

In this work, a recombinant plum pox virus (PPV, Sharka) encoding green fluorescent protein is used to study its effect on antioxidant enzymes and protein expression at the subcellular level in pea plants (cv. Alaska). PPV had produced chlorotic spots as well as necrotic spots in the oldest leaves at 13–15 d post-inoculation. At 15 d post-inoculation, PPV was present in the chlorotic and necrotic areas, as shown by the fluorescence signal produced by the presence of the green fluorescent protein. In the same areas, an accumulation of reactive oxygen species was noticed. Studies with laser confocal and electron microscopy demonstrated that PPV accumulated in the cytosol of infected cells. In addition, PPV infection produced an alteration in the chloroplast ultrastructure, giving rise to dilated thylakoids, an increase in the number of plastoglobuli, and a decreased amount of starch content. At 3 d post-inoculation, although no changes in the oxidative stress parameters were observed, an increase in the chloroplastic hydrogen peroxide levels was observed that correlated with a decrease in the enzymatic mechanisms involved in its elimination (ascorbate peroxidase and peroxidase) in this cell compartment. These results indicate that an alteration in the chloroplastic metabolism is produced in the early response to PPV. This oxidative stress is more pronounced during the development of the disease (15 d post-inoculation) judging from the increase in oxidative stress parameters as well as the imbalance in the antioxidative systems, mainly at the chloroplastic level. Finally, proteomic analyses showed that most of the changes produced by PPV infection with regard to protein expression at the subcellular level were related mainly to photosynthesis and carbohydrate metabolism. It seems that PPV infection has some effect on PSII, directly or indirectly, by decreasing the amount of Rubisco, oxygen-evolving enhancer, and PSII stability factor proteins. The results indicate that Sharka symptoms observed in pea leaves could be due to an imbalance in antioxidant systems as well as to an increased generation of reactive oxygen species in chloroplasts, induced probably by a disturbance of the electron transport chain, suggesting that chloroplasts can be a source of oxidative stress during viral disease development.

Key words: 2D electrophoresis, oxidative stress, *Pisum sativum* L., plum pox virus, sharka.

Introduction

Sharka, a disease caused by plum pox virus (PPV), is a serious limiting factor for temperate fruit production in affected areas, resulting in severe economic losses in *Prunus* species including apricot and peach (Kölber, 2001). PPV also infects herbaceous plants such as *Nicotiana clevelandii*, *N. benthamiana*, and *Chenopodium*

* To whom correspondence should be addressed. E-mail: jahernan@cebas.csic.es

Abbreviations: APX, ascorbate peroxidase; CP, coat protein; DHAR, dehydroascorbate reductase; dpi, days post-inoculation; G6PDH, glucose-6P-dehydrogenase; GFP, green fluorescent protein; GPX, glutathione peroxidase; GR, glutathione reductase; GST, glutathione *S*-transferase; H_2O_2, hydrogen peroxide; MDHAR, monodehydroascorbate reductase; NPQ, non-photochemical quenching; O_2^-, superoxide radical; OEE, oxygen-evolving enhancer; OPPP, oxidative pentose phosphate pathway; *p*HMB, *p*-hydroxymercuribenzoic acid; POX, peroxidase; PPV, plum pox virus; PSII, photosystem II; q_p, photochemical quenching coefficient; ROS, reactive oxygen species; SOD, superoxide dismutase.

foetidum (Van Oosten, 1971; Németh, 1986). These species have been used as indicator plants in detection and localization studies (Martínez-Gómez and Dicenta, 2001). Some pea cultivars, such as cv. Colmo and cv. Alaska, have been described as very susceptible to PPV (Morvan and Chastelliere, 1980). However, until now, almost no data about the biochemical and physiological responses of PPV-susceptible herbaceous plants to PPV infection have been available in the scientific literature. The only published information about the effect of PPV infection on some biochemical parameters from susceptible herbaceous plants is limited to some changes in the isozyme profile of peroxidase (POX), glutamate oxalacetate transaminase, and estereases in *C. foetidum* and *N. clevelandii* (Visedo *et al*., 1990, 1991).

In some compatible virus–host plant interactions, an oxidative stress is produced (Riedle-Bauer, 2000; Clarke *et al*., 2002; Hernández *et al*., 2004, 2006; Díaz-Vivancos *et al*., 2006). In previous work it was observed that PPV infection produced an oxidative stress only in susceptible *Prunus* species, manifested as an increase in different oxidative stress parameters (lipid peroxidation, protein oxidation, and electrolyte leakage), accumulation of hydrogen peroxide (H_2O_2), and an imbalance in the antioxidative systems at the subcellular level. These effects were not produced in a resistant apricot cultivar, where the PPV inoculation did not produce any effect on the oxidative stress parameters and some antioxidant enzymes even increased in soluble fractions and in the apoplastic space (Díaz-Vivancos *et al*., 2006; Hernández *et al*., 2006). However, different factors, including the use of woody plants, the mode of inoculation and the time which passed between the subjection of the plants to artificial dormancy and the growth of the first expanding leaves (Martínez-Gómez and Dicenta, 2000), made it difficult to study the early responses to PPV infection, and results were obtained for long-term PPV infection (Hernández *et al*., 2001*b*, 2004, 2006; Díaz-Vivancos *et al*., 2006). So, the use of a PPV-susceptible herbaceous plant can permit the study of the biochemical and physiological effects of PPV infection in a shorter term than for *Prunus* plants.

Recombinant green fluorescent protein (GFP)-tagged viruses have been used intensively to study viral invasion in different plant/virus pathosystems. Recently, different authors have used the recombinant PPV-encoding GFP to study the plant–PPV interaction in *Prunus* and *Nicotiana* species (Lansac *et al*., 2005; Alamillo *et al*., 2006).

High-throughput proteomic analysis is a powerful tool to study changes in accumulation levels and post-translational modifications of proteins in particular tissues under given conditions (Campo *et al*., 2004). In plants, the proteomic approach has been employed to study alterations in cellular protein content in response to various biotic and abiotic stresses (Campo *et al*., 2004; Dani *et al*., 2005; Casado-Vela *et al*., 2006; Díaz-Vivancos *et al*., 2006). Moreover, subcellular fractionation provides information about protein localization and allows new insights into pathway compartmentalization and protein sorting (Baginsky and Gruissem, 2004).

In the present work, using a GFP-tagged recombinant virus, the physiological and biochemical responses of pea plants to PPV infection are studied over a shorter time than would be the case with woody plants. Changes in the antioxidant systems and protein expression were analysed at the subcellular level. In addition, the distribution of the virus was analysed by using different detection techniques, in order to deepen our knowledge of the plant–PPV interaction.

Materials and methods

Plant material

Pea (*Pisum sativum* L cv. Alaska.) seeds were surface-sterilized (10%, v/v, sodium hypochlorite for 2 min), germinated, and grown in vermiculite. Vigorous seedlings were selected for hydroponic culture in a growth chamber. Plants were cultivated in aerated distilled water for 7 d and then were transferred to aerated half-strength Hoagland solution (Hernandez *et al*., 1995; Martínez-Cordero *et al*., 2005) for the rest of the experiment. The growth chamber was set at 25/18 °C, 80% relative humidity, and a 16/8 h photoperiod at a light intensity of 200 μmol m^{-2} s^{-1}.

GFP-tagged recombinant PPV isolate

Recombinant PPV encoding GFP (PPVPSI4-RnGFPs, derived from a Marcus-type isolate) (B Salvador *et al*., unpublished results) was used to inoculate the pea plants. This isolate is kept in the Centro Nacional de Biotecnología (CNB-CSIC), Madrid (Spain).

Plant inoculation

Plants were inoculated on the 5th day after addition of the half-strength Hoagland solution. The first inoculum source used in this work was *Nicotiana benthamiana* plants infected with PPVPSI4-RnGFPs. Later, infected pea plants were used for the following inoculations. The infected plants, used as inoculum source, were homogenized (1/2 w/v) in K-phosphate buffer, pH 7.2, containing benthonite. The crude homogenate was filtered through two layers of cheesecloth and directly used for mechanical inoculation of pea seedlings, using carborundum. Controls were mock-inoculated by using a crude extract from non-inoculated pea leaves. Plants were analysed at the initiation phase [3 d post-inoculation (dpi), early response] and the elaboration phase (15 dpi, disease development).

PPV detection

An ELISA-DASI (double antibody sandwich indirect) test was applied to the leaves, using the 5B-IVIA monoclonal antibody against the coat protein (CP) of PPV (Durviz, Madrid, Spain) (Hernández *et al*., 2004). For the detection of PPV nucleic acid, an RT-PCR analysis was carried out using total RNA extracted using the RNeasy Plant Mini Kit (Qiagen, Hilden, Germany). Two specific primers within the CP gene, VP337 (CTCTGTGTCCTCTTCTTGTG), complementary to positions 9487–9508 of genomic PPV RNA, and VP338 (CAATAAAGCCATTGTTGGATC), homologous to positions 9194–9216, were used. The PCR parameters

were: one cycle at 94 °C for 2 min, followed by 30 cycles of 94 °C for 30 s, 55 °C for 30 s, and 72 °C for 30 s, and finally an extension step at 72 °C for 5 min. Amplified products were electrophoresed in 1% agarose gels, in 40 mM TRIS-acetate and 1 mM EDTA, pH 8.0, and stained with ethidium bromide.

Fluorescence measurements

Ten control and PPV-infected pea plants were analysed in every experiment. Modulated chlorophyll fluorescence was measured in dark-adapted pea leaves at midday, using a chlorophyll fluorometer OS-30 (Optisciences, USA) with an excitation source intensity of 2000 μmol m^{-2} s^{-1}. The quantum yield of photosystem II (PSII) photochemistry (Φ_{PSII}), the maximum quantum yield of PSII (F_v/F_m), the non-photochemical quenching (NPQ), and the photochemical quenching coefficient (q_p) were calculated as described previously (Hernández *et al*., 2004). The efficiency of excitation energy capture by PSII, corresponding to the probability that an absorbed photon reaches the PSII reaction centres, was calculated in light-adapted leaves as $F'_v/F'_m=(F'_m–F'_o)/F'_m$. The minimal 'dark' fluorescence level following illumination (F'_o) was measured in the presence of a background far-red light, to favour rapid oxidation of intersystem electron carriers.

Isolation of cell fractions

For the isolation of cell fractions, 3 dpi and 15 dpi pea plants were used. At 3 dpi all the leaves of the pea seedling were used. At 15 dpi only systemic leaves showing symptoms were used, and similar leaves were used in control plants. All operations were carried out at 0–4 °C. Soluble fractions were obtained from pea leaves (15 g) by differential centrifugation according to published protocols (Hernández *et al*., 2004, 2006). For ascorbate peroxidase (APX) activity, 20 mM ascorbate was added. The resulting supernatant was partially purified in Sephadex G-25 NAP columns (GE Healthcare, Madrid, Spain) equilibrated with 50 mM K-phosphate buffer pH 7.0 (with or without 2 mM ascorbate), and was considered as the soluble fraction for use in different assays. Chloroplasts were isolated by differential and density-gradient centrifugation (Hernández *et al*., 2004). A resuspension medium containing 20% (v/v) Percoll (GE Healthcare) was layered under the chloroplast suspension, by slowly pipetting 10 ml into the bottom of the tube. Tubes were centrifuged at 1700 *g* for 1 min. The pellet of intact chloroplasts was resuspended in 1 ml of washing medium, without BSA, and used for enzyme assays. Chloroplasts were lysed by incubation (v/v) with 10 mM K-phosphate buffer, pH 7.0, containing 0.2% (v/v) Triton X-100, for 1 h. After incubation, the lysed chloroplast preparations were centrifuged at 100 000 *g* for 15 min (Optima Max ultracentrifuge, Beckman, USA) and the supernatants obtained were partially purified in Sephadex G-25 NAP columns (GE Healthcare) equilibrated with 50 mM K-phosphate buffer pH 7.0 (with or without 2 mM ascorbate).

Enzymatic assays

Catalase, superoxide dismutase (SOD), POX, the ascorbate-glutathione cycle enzymes as well as the glucose-6P-dehydrogenase (G6PDH) activity were measured as described in Hernández *et al*. (2000, 2001*b*, 2004). APX was measured in the presence and absence of the specific inhibitor *p*-hydroxymercuribenzoic acid (*p*HMB; 0.5 mM). pHMB-sensitive APX activity was considered as due to class I APX, whereas pHMB-insensitive APX activity is due to a class III POX that can use ascorbate as reducing power (Hernández *et al*., 2004). Glutathione peroxidase (GPX) activity was determined by measuring the formation of oxidized glutathione coupled to the oxidation of NADPH, at 340 nm, carried out by commercial glutathione reductase (GR; Sigma) according to Overbaugh and Fall (1985). Glutathione *S*-transferase (GST) activity was analysed according to Habing and Jakoby (1981), based on the increase of absorbance at 340 nm due to the formation of a conjugated compound by the reaction of GSH with 1-chloro-2,4-dinitrobenzene.

Determination of H_2O_2 and oxidative stress parameters

The measurement of H_2O_2 contents in soluble fractions and chloroplasts was based on the peroxide-mediated oxidation of Fe^{2+}, followed by the reaction of Fe^{3+} with xylenol orange (Bellicampi *et al*., 2000). The extent of lipid peroxidation and protein oxidation (carbonyl-protein content) in pea leaves was estimated as described in Hernandez *et al*. (2004). Electrolyte leakage in pea leaves was measured as described previously (Diaz-Vivancos *et al*., 2006).

Histochemical detection of H_2O_2 and superoxide radicals (O_2^-) in pea leaves

The histochemical detection of H_2O_2 in pea leaves was performed using endogenous POX-dependent *in situ* histochemical staining, in which whole leaves were vacuum-infiltrated with 0.1 mg ml^{-1} 3, 3′-diaminobenzidine in 50 mM TRIS-acetate buffer (pH 5.0) and incubated at 25 °C, in the dark, for 24 h. Controls were performed in the presence of 10 mM ascorbic acid (Hernández *et al*., 2001*a*). The histochemical detection of O_2^- was performed by infiltrating leaf quarters directly with 0.1 mg ml^{-1} NBT in 25 mM K-HEPES buffer (pH 7.6) and incubating at 25 °C in the dark for 2 h (Hernández *et al*., 2001*a*). In both cases, leaves were rinsed in 80 % (v/v) ethanol for 10 min at 70 °C, mounted in lactic acid:phenol:-water (1:1:1, v/v/v), and photographed directly using an Olympus SZX PT stereomicroscope.

Fluorescence microscopy

The *in vivo* analysis of GFP protein in infected pea leaves was performed with a fluorescence stereomicroscope (Leica MZ FLIII), using a fluorescence filter for GFP at 425/60 nm excitation and a 480 nm blockade. The images were captured with a digital camera (Leica DL500) attached to the magnifying lens.

Confocal laser microscopy

A Leica TCS SP2 laser confocal microscope (Leica Microsystem Heidelberg GmbH) was used for GFP localization in pea leaves infected with the GFP-tagged PPV. The excitation energy was produced by an argon laser at 488 nm, and the band in the range 505–525 nm was observed. A pinhole of 120 nm was used. For the cellular localization of the GFP-tagged PPV, Normansky microscopy was used. Afterwards, the images were analysed using the system's own software.

Transmission electron microscopy

For microscopy, samples were fixed for 2.5 h, at 4 °C, in a 0.1 M Na-phosphate-buffered (pH 7.2) mixture of 2.5% glutaraldehyde and 4% paraformaldehyde (Morales *et al*., 2001). Tissue was post-fixed with 1% osmium tetroxide, for 2 h. The samples were then dehydrated in a graded alcohol series and embedded in Spurr's resin. Blocks were sectioned on a Reichert ultramicrotome (Germany). Thin sections for transmission electron microscopy were placed on copper grids and stained with uranyl acetate, followed by lead citrate. The ultrastructure of the tissue was observed with a Philip Tecnai electron microscope (Germany).

Electrophoretic analyses

Soluble fractions or lysed chloroplasts were subjected to a cleaning procedure by using the CleanUp kit® (Madrid, Spain). The proteins

obtained were resuspended in Destreak™ rehydration solution (GE Healthcare, Madrid, Spain) containing Destreak Reagent (GE Healthcare). For 2D electrophoresis, proteins were separated initially according to isoelectric focusing in the first dimension. Isoelectric focusing was carried out using 150 µg samples of soluble fractions or chloroplastic proteins, in gel strips with an immobilized linear pH gradient of 4–7 (Bio-Rad) (Diaz-Vivancos *et al*., 2006). The second dimension (SDS-PAGE) was performed as described previously (Díaz-Vivancos *et al*., 2006). Gels were stained with Bio-Safe™ Coomassie G-250 (Bio-Rad). Experiments were carried out three times. Gels were scanned and analysed by using the PDQuest software (Bio-Rad). Spots, where intensity increased or decreased strongly (3-fold), were excised from the gels, and identified by MALDI-TOF and ion trap analysis in the Spanish National Cancer Research Centre (CNIO, Madrid, Spain).

Results

PPV localization and cell structure modifications associated with PPV infection

Sharka symptoms appeared in pea leaves at 13–15 dpi, and consisted of chlorotic spots in systemic leaves as well as necrotic spots in the oldest systemic leaves (Fig. 1). In addition, PPV presence in leaves was confirmed by an ELISA-DASI test (presence of PPV CP) and RT-PCR analysis (presence of PPV nucleic acid). At 3 dpi, plants were weakly RT-PCR positive, showing a weak band corresponding to the nucleic acid amplification of the virus (not shown). However, at 15 dpi, a strong band corresponding to the nucleic acid of the virus was observed, confirming that the number of virus particles increased with the time of infection (data not shown). In the same way, the ELISA test correlated with the data obtained by RT-PCR. At 3 dpi, only some inoculated plants were ELISA-positive (considering 'positive' as double the absorbance obtained with control, non-infected samples) (Table 1). However, at 15 dpi, infected leaves were strongly ELISA-positive, showing an optical density increase of 40-fold, relative to control leaves (Table 1).

At 15 dpi, the observation of infected leaves proved that PPV was present in the chlorotic and necrotic areas, as shown by the fluorescence signal produced by the presence of the GFP (see Fig. 2C, D, in relation to the control shown in A, B). The chlorotic symptoms appeared near the minor veins and in the same areas accumulation of H_2O_2 and $O_2^{\cdot-}$, detected by histochemical analyses, was noticed (in Fig. 3 compare B, C with controls shown in A, D). H_2O_2 accumulation appeared as a red-brown staining due to diaminobenzidine polymerization in the presence of H_2O_2 and endogenous POX (Fig. 3B). This staining seemed to be due to H_2O_2 since it was totally suppressed by 10 mM ascorbic acid (Fig. 3C). Superoxide accumulation appeared as a dark-blue staining due to the reduction of NBT by $O_2^{\cdot-}$ (Fig. 3E).

The confocal laser microscopy studies demonstrated the distribution of the GFP signal in the cytosol of the infected cells, near the cell wall (in Fig. 4 compare B, E with the control in D), which suggests the presence of PPV in this compartment. Likewise, its presence was observed in the vascular bundles in the associated cells

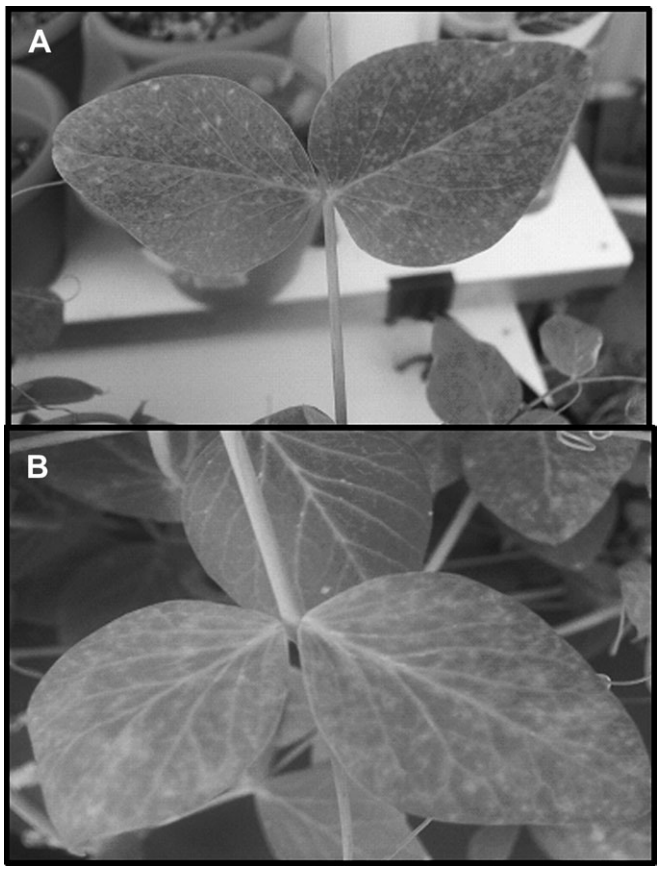

Fig. 1. Sharka symptoms in PPV-infected plants in the phase of disease development (15 dpi): (A) infected plants showing chlorotic spots; (B) infected plants showing necrotic spots in the oldest leaves.

Table 1. *PPV detection in inoculated and control pea (cv. Alaska) plants*

Number of plants giving positive results by ELISA and/or RT-PCR analysis. In the initial phase of the infection process (3 dpi), both inoculated and systemic leaves were assayed. In the phase of disease development (15 dpi), only systemic leaves were analysed.

	Evaluated plants	Symptoms[a]	ELISA[b]	RT-PCR
3 DPI				
Control	10	0	– (0.139)	–
Inoculated	10	0	± (0.220–0.280)	+
15 DPI				
Control	10	0	– (0.101)	–
Inoculated	10	5	+ (3.980)	+

[a] Symptoms intensity on a scale from 0 (no symptoms) to 5 (maximum intensity).
[b] Mean optical density of ELISA at 405 nm, after 60 min.

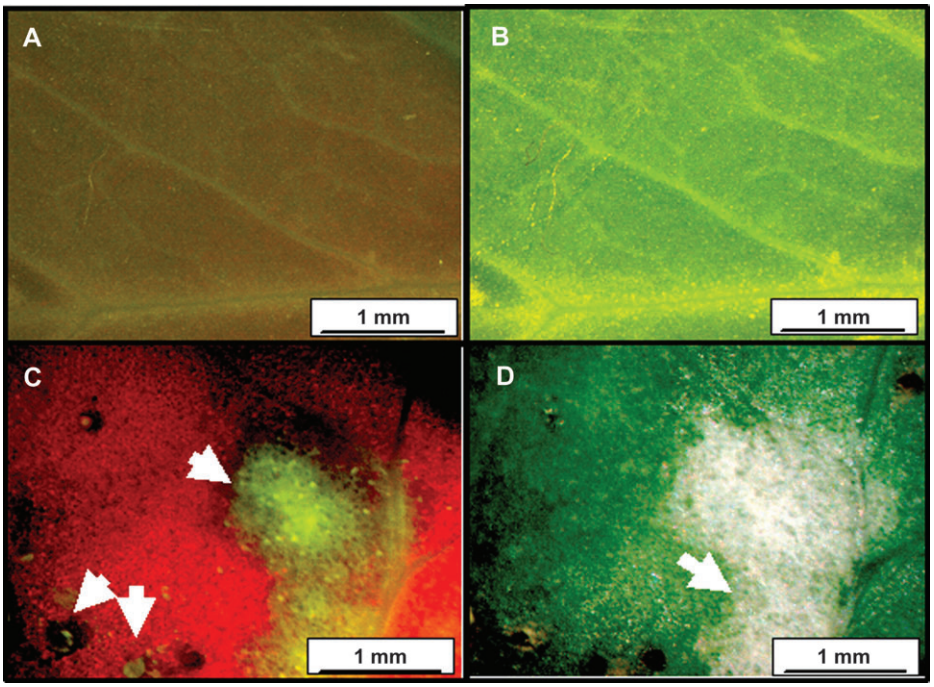

Fig. 2. Localization of PPV (PPVPSI4-RnGFPs) expressing GFP in pea leaves, under a fluorescence microscope (A, C) in the chlorotic areas, under visible light (B, D). Control plants (A, B); PPV-inoculated plants (C, D). Arrows show the fluorescence signal produced by the presence of the GFP in the chlorotic area (central arrow in Fig. 3C) and in the necrotic areas (left bottom corner in Fig. 3C). Pea leaves in the phase of disease development (15 dpi) were used.

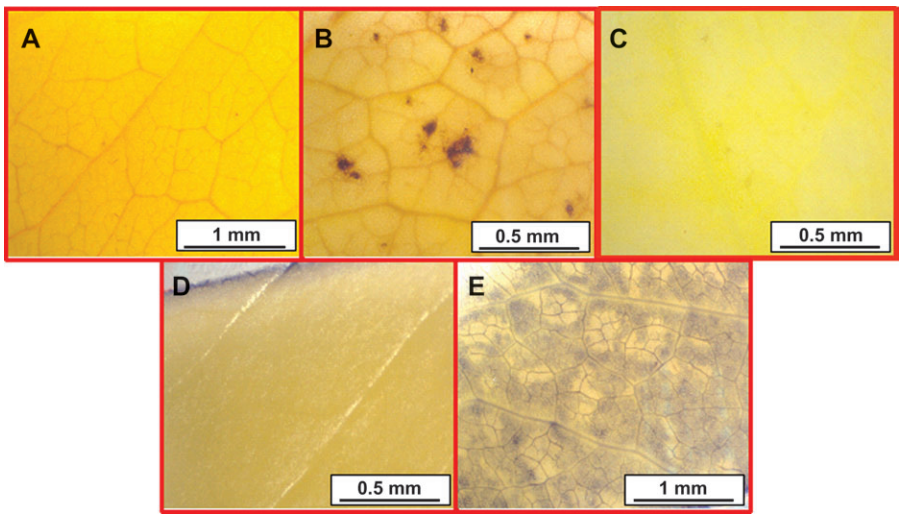

Fig. 3. Effect of PPV infection on H_2O_2 (A, B, C) and O_2^- (D, E) accumulation in pea leaves, detected by histochemical staining with DAB and NBT, respectively. (A) DAB-staining of a control pea leaf; (B) DAB-staining of a PPV-infected pea leaf; (C) DAB-staining of a PPV-infected pea leaf in the presence of ascorbate; (D) NBT-staining of a control pea leaf; (E) NBT-staining of a PPV-infected pea leaf. Pea leaves in the phase of disease development (15 dpi) were used.

(parenchyma and transfer cells) but not in the xylem vessels (compare C and F in Fig. 4).

As mentioned above, PPV appeared to infect all cell types (Fig. 5A, E, F, G, H), but it was not present in the sieve tube elements nor in the xylematic vessels (Fig. 5D). The virus was present mainly in transfer cells and parenchymatic cells (Fig. 5A, D, G). PPV appeared as pinwheel-shaped cytoplasmic inclusions, typical of potyviral infections (Riedel *et al*., 1998) (Fig. 5E, F). Likewise, viral particles were also observed in the cytosol (Fig. 5G, I). When these structures were near the cell wall they were oriented perpendicularly and, in some cases,

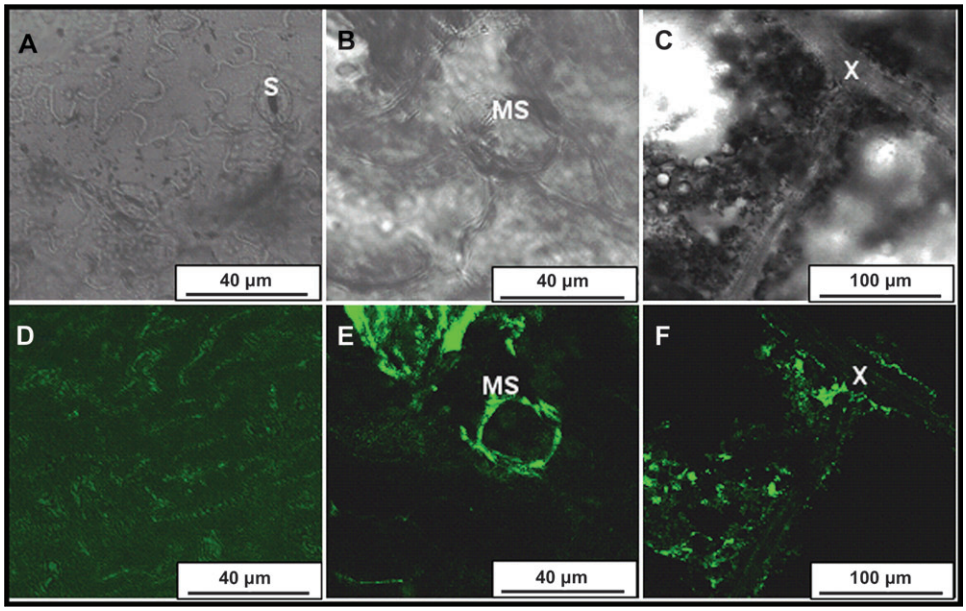

Fig. 4. Images taken under a laser confocal microscope of pea leaves systemically infected with PPV: control leaves as negative control (D); DIC (differential interference contrast) image showing stomata (A); detail of mesophyll cell showing the presence of the GFP signal in the cytoplasm (E); DIC image of same cell (B); vascular bundle showing a positive location of the virus (F); and DIC image of the same area (C). S, Stomata; MS, mesophyll cell; X, xylem. Pea leaves in the phase of disease development (15 dpi) were used.

their presence was detected near the plasmodesmata (Fig. 5I). Chloroplasts from cells associated with the vascular system were affected most by PPV infection; they had dilated thylakoids, lower starch content, and a higher number of plastoglobuli (Fig. 5B) in relation to chloroplasts from control plants (Fig. 5C). However, chloroplasts from other cell types (i.e. mesophyll cells) showed less damage (not shown).

Biochemical and physiological effects of PPV infection in pea

At 3 dpi, no significant changes in fluorescence parameters due to the effect of PPV inoculation were observed (data not shown). At 15 dpi, no evident changes in the PSII efficiency (F_v/F_m), the efficiency of excitation energy capture by PSII (F'_v/F'_m), the quantum yield of PSII electron transport (Φ_{PSII}), or the photochemical quenching coefficient (q_p) were produced. However, a decrease in the NPQ parameter was noticed (Table 2). The decrease in NPQ was parallel to a decrease in the chlorophyll contents in isolated chloroplasts at 15 dpi (0.54 and 0.35 mg chlorophyll ml^{-1}, from control and PPV-infected plants, respectively).

In the initiation phase of infection (3 dpi), no changes in the oxidative stress parameters were produced (data not shown), although an increase in H_2O_2 levels was observed in the chloroplasts from inoculated plants (Fig. 6A). This effect can be considered as the early response to PPV in pea plants. However, in the disease development phase (15 dpi), PPV infection produced an oxidative stress in pea leaves as reflected by the increase in lipid peroxidation, protein oxidation, and electrolyte leakage, as well as the increase in H_2O_2 levels in soluble fractions and chloroplasts from infected leaves (Figs 6, 7). The increase in H_2O_2 levels correlated with the observed H_2O_2 and $O_2^{\cdot-}$ accumulation detected by histochemical analyses (Fig. 3).

PPV infection also produced an alteration in the levels of antioxidant enzymes in the soluble fractions and chloroplasts from pea leaves. At 3 dpi, PPV inoculation produced a drop in APX as well as an increase in POX activity in the soluble fractions. In chloroplasts, the observed increase in H_2O_2 correlated with a fall in APX and POX. Also, an increase in G6PDH was observed in chloroplasts from inoculated plants (Table 3).

More changes in the levels of antioxidant enzymes due to the effect of PPV infection were apparent at 15 dpi than at 3 dpi. In soluble fractions, increases in POX, APX, and *p*HMB-insensitive APX, as well as decreases in catalase and GST, were observed. In chloroplasts, PPV infection produced a decrease in GPX, GR, and SOD as well as an increase in monodehydroascorbate reductase (MDHAR) (Table 4).

Changes in the pea proteome associated with PPV infection

In order to study the effect of PPV infection on the differential protein expression at a subcellular level, a proteomic approach was applied. This proteomic approach was carried out in chloroplast and soluble fractions from pea leaves in the initiation phase of PPV infection (early

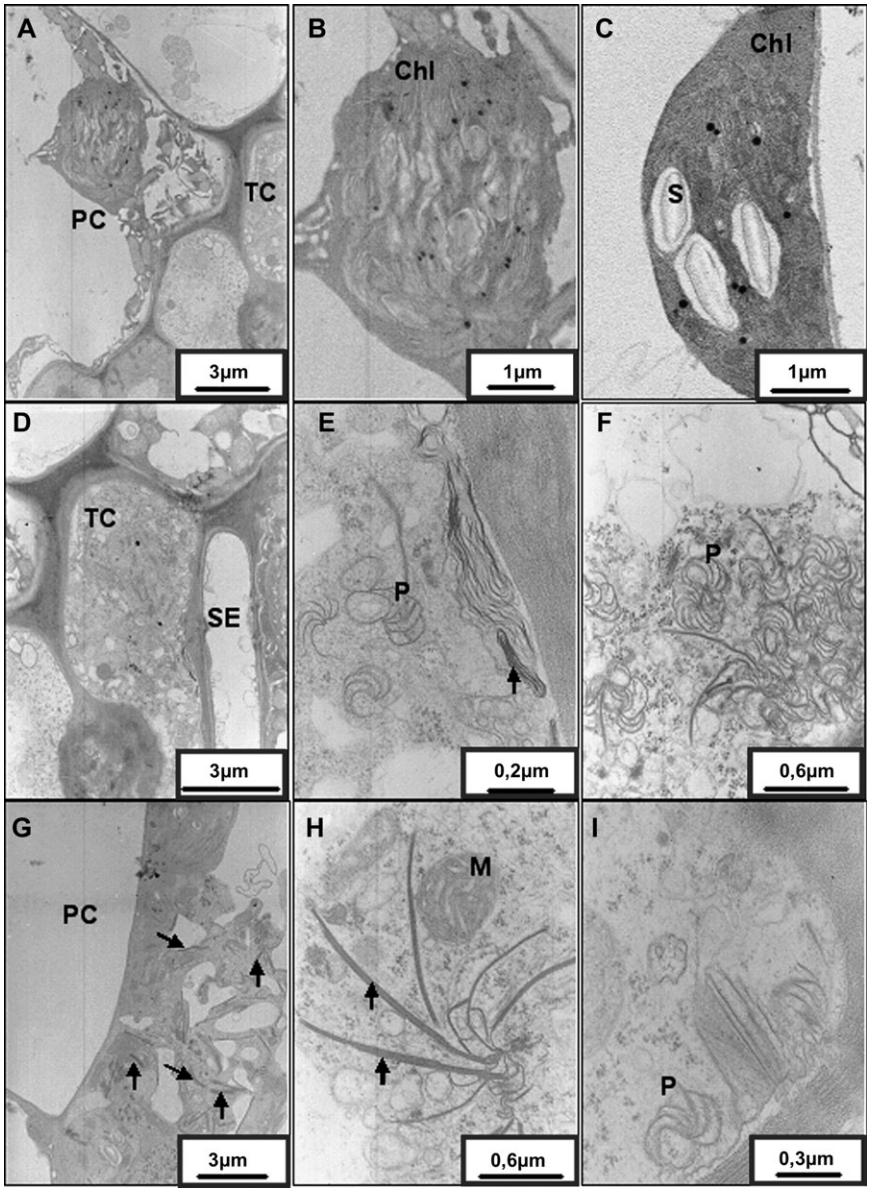

Fig. 5. Transmission electron microscopy of *Pisum sativum* leaves infected with PPV in the phase of disease development (15 dpi). (A) Parenchymatic cell from a PPV-infected vascular bundle. (B) Detail of the previous micrograph showing a chloroplast with dilated thylakoids. (C) Detail of a chloroplast from a non-infected plant. (D) Transfer cells from a PPV-infected vascular bundle. (E) Detail of the previous micrograph, showing abundant pinwheels in the cytoplasm and cytoplasm lamellar bodies close to the cell wall (arrow). (F) Detail of cytoplasm from an infected parenchymatic cell showing abundant pinwheels. (G) Parenchymatic cell with abundant virus particles in the cytoplasm (arrows). (H) Detail of an infected parenchymatic cell showing virus particles in the cytoplasm (arrows). (I) Detail of a transfer cell showing a pinwheel and virus particles perpendicular to the cell wall. Chl, Chloroplast; M, mitochondria; P, pinwheels; PC, parenchymatic cell; S, starch grain; SE, sieve tube element; TC, transfer cell.

response, 3 dpi) and in the elaboration phase (disease development, 15 dpi).

Soluble fractions showed some chloroplastic contamination. In previous work, it was estimated that in pea plants the degree of chloroplastic contamination in soluble fractions is around 20% (Hernández *et al*., 2000). The contamination was much higher in soluble fractions from PPV-infected leaves than in control leaves. This proves that chloroplasts from infected plants had a higher degree of membrane damage, which correlated with the increased H_2O_2 levels detected in chloroplasts.

After 2D gel electrophoresis analyses, the spots where expression increased or decreased strongly (3-fold) were selected (Figs 8, 9; Tables 5, 6). Ion trap analysis provided additional data about proteins that were not identified by peptide mass fingerprint. Thus, at 3 dpi, some spots not identified by MALDI-TOF (spots 33, 34, 40, 41, 43, and 48 in the soluble fraction and spot 27 in the chloroplastic

Table 2. *Fluorescence parameters measured in control and PPV-infected pea leaves in the phase of disease development (15 dpi)*

Data represent the means ±SE from 10 repetitions. Differences from control values are significant at $P < 0.05$ (a), according to Duncan's multiple range test.

Fluorescence parameters	Control plants	PPV-infected plants
F_v/F_m	0.874±0.006	0.856±0.007
F'_v/F'_m	0.838±0.003	0.837±0.003
Φ_{PSII}	0.114±0.008	0.108±0.007
q_p	0.145±0.010	0.134±0.009
NPQ	0.170±0.010	0.116±0.007 a

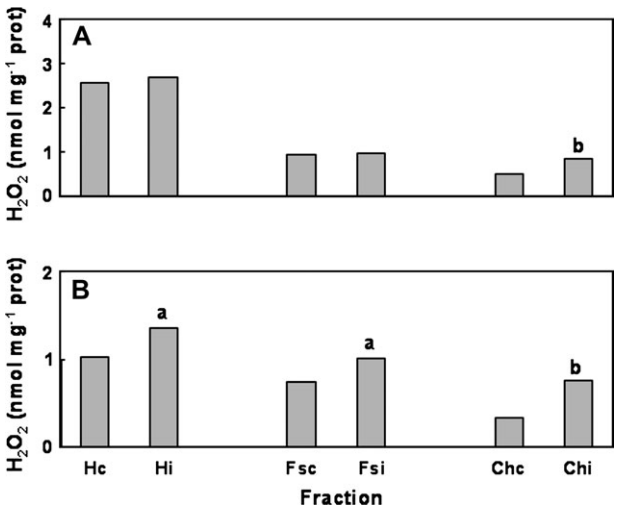

Fig. 6. Effect of PPV infection on H_2O_2 contents in different cell fractions from pea leaves during the initiation (3 dpi, early response) (A) and the elaboration (15 dpi, disease development) (B) phases of disease development. Hc, Homogenate from control leaves; Hi, homogenate from inoculated leaves; Fsc, soluble fraction from control leaves; Fsi, soluble fraction from inoculated leaves; Chc, chloroplast from control leaves; Chi, chloroplast from inoculated leaves. Data represent the means ±standard errors of at least 3 replicates. Differences from control values were significant at $P < 0.05$ (a) and $P < 0.01$ (b) according to Duncan's multiple range test.

fraction) (Fig. 8; Table 5) were identified by means of ion trap analysis, and in the soluble fraction PPV produced a decrease in all these polypeptides (Table 5). In the early response to PPV, transketolase (spots 33 and 34 in Fig. 8), an enzyme involved in both the oxidative pentose phosphate pathway (OPPP) and the Calvin cycle, decreased by effect of infection. Interestingly, spots corresponding to the same protein were enhanced by PPV infection at 15 dpi (spots 8 and 9 in Fig. 9; Table 6). A spot corresponding to the PPV CP (spot 23) was only observed in the soluble fraction from infected plants in the phase of disease development but not during the initiation phase (Fig. 9; Table 6).

PPV produced an alteration in some polypeptides related with the photosynthetic process. At 3 dpi, decreases in Rubisco (spot 13) and oxygen-evolving enhancer (OEE) complex (spot 28) (Table 5; Fig. 8) were noticed in the chloroplastic fraction. At 15 dpi, a decrease in Rubisco (spots 31, 33, 34, 35, and 36) as well as in three polypeptides showing homology with the OEE complex was also observed (38, 39, and 40) (Table 6; Fig. 9). In addition, a fall in a polypeptide with homology to the PSII stability factor was produced (spot 37 in Fig. 9; Table 6). Finally, in chloroplasts from 15 dpi plants, PPV increases aldolase (spots 47 and 48 in Fig. 9; Table 6).

Discussion

The pea cultivar Alaska is very susceptible to PPV, as shown by the strong chlorosis symptoms observed at 15 dpi. At 3 dpi, no symptoms were observed and ELISA and RT-PCR showed a weak presence of the virus. The microscopy studies demonstrated the presence of PPV in the vascular-associated cells but not in the sieve elements or the xylematic vessels (Figs 4, 5). In *in vitro* peach cv. GF305 infected with a GFP-tagged PPV, the GFP signal was visible in the cytoplasm, near the cell wall of mesophyll and epidermal cells (Lansac *et al*., 2005). In PPV-infected pea plants, the GFP signal was clearly associated with chlorosis symptoms as well as with ROS generation; this was also observed in PPV-infected peach and tobacco plants. However, both in peach and in tobacco plants, the PPV-associated fluorescence was found in the vascular vessels (Lansac *et al*., 2005; Alamillo *et al*., 2006). These differences could be due to different factors, including the different plant species used, the PPV clone, and the inoculation methods—tobacco plants were inoculated by infiltration with *Agrobacterium tumefaciens* (Alamillo *et al*., 2006), whereas *in vitro* peach plants were inoculated by shoot tip grafting (Lansac *et al*., 2005).

In the phase of disease development (15 dpi), PPV produced some ultrastructural alterations in infected pea plants, mainly in chloroplasts. These alterations correlated with the decrease in NPQ, the accumulation of chloroplastic H_2O_2, and the imbalance of chloroplastic antioxidant systems. These effects on chloroplast ultrastructure seem to be a general stress response, because they have been described previously, both under biotic and abiotic stress conditions (Hernández *et al*., 1995, 2004, 2006; Morales *et al*., 2001).

The levels of lipid peroxidation, protein oxidation, and electrolyte leakage, as well as ROS accumulation, are oxidative stress parameters commonly used to assess the extent of cell damage produced under different stress situations (Hernández *et al*., 1995, 2001*a*; Díaz-Vivancos *et al*., 2006). At 15 dpi, PPV infection produced an oxidative stress in pea plants as observed by the increases in some oxidative stress parameters in leaves (Fig. 7). By contrast, in the initiation phase of the infection process

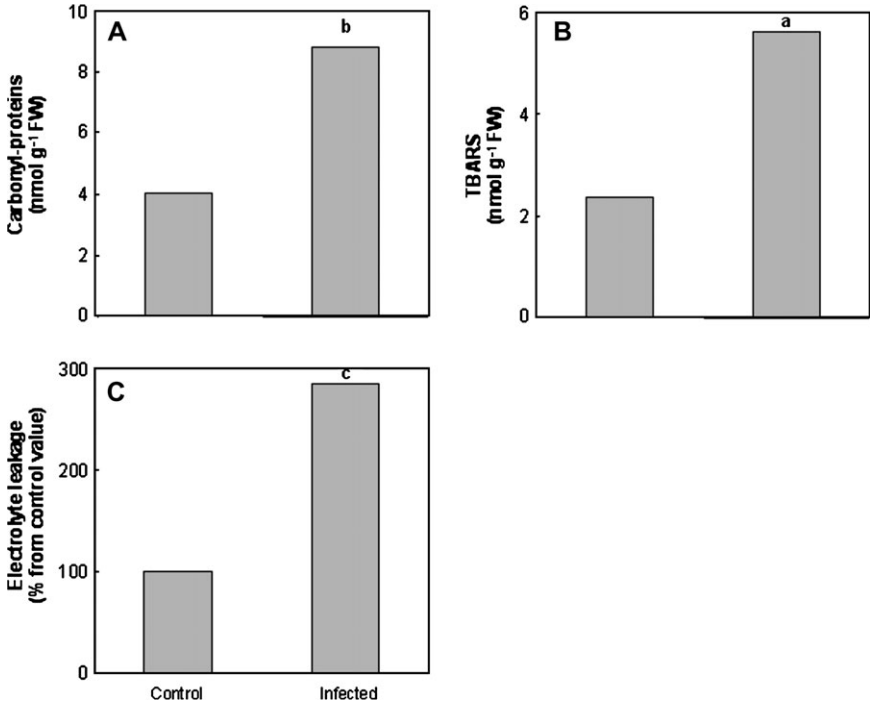

Fig. 7. Effect of PPV infection on some oxidative stress parameters of pea plants in the phase of disease development (15 dpi). (A) Protein oxidation (measured as carbonyl-proteins); (B) lipid peroxidation (measured as TBARS); (C) electrolyte leakage. Data represent the means ±standard errors of at least three replicates. Differences from control values were significant at $P < 0.05$ (a), $P < 0.01$ (b), or $P < 0.001$ (c), according to Duncan's multiple range test. Control or Infected in (A) and (B); *x*-axis as in (C).

(3 dpi), although no changes were observed in the oxidative stress or in the fluorescence parameters, an increase in H_2O_2 took place in the chloroplasts but not in the soluble fractions (Fig. 6). This observation indicates that an alteration in the chloroplastic metabolism is produced in the early response to PPV.

The observed oxidative stress produced by the PPV infection was correlated with changes in the antioxidative system of pea plants at the subcellular level. Changes were more prominent at 15 dpi than at 3 dpi. The chloroplastic H_2O_2 accumulation at 3 dpi correlated with a decrease in the enzymatic mechanisms involved in H_2O_2 elimination in this cell compartment (POX and APX activities) (Table 3). At 15 dpi, although an important increase in H_2O_2-scavenger enzymes took place in the soluble fractions (*p*HMB-sensitive APX, *p*HMB-insensitive APX, and POX), H_2O_2 accumulated in this fraction. In parallel, a drop in catalase was detected (Table 4). A decrease in catalase activity was also described in PPV-infected apricot leaves (Hernández *et al*., 2006) and in *Tobacco mosaic virus* (TMV)-infected *Nicotiana glutinosa* L. plants (Yi *et al*., 1999). In higher plants, catalase is localized mainly in peroxisomes (del Río *et al*., 1998). The decrease in catalase observed in the phase of disease development (15 dpi) could have contributed to an increase in peroxisomal H_2O_2, that could also have diffused through the peroxisomal membrane into the cytosol (del Río *et al*., 1998), thus contributing to the detected H_2O_2 accumulation in the soluble fraction and increasing the risk of oxidative damage. A strong decrease in catalase has also been described in peroxisomes from senescent leaves, suggesting a role for peroxisomes in the oxidative mechanisms of leaf senescence (del Rio *et al*., 1998). Increased lipid and protein oxidation was seen in PPV-infected pea leaves at this stage, which could also indicate senescence. So, a possible role for peroxisomes as a putative source of ROS generation during the phase of disease development could also be suggested.

There are an increasing number of studies using proteomic approaches to study metabolic changes in response to different environmental stresses. For example, the effect of TMV infection in tomato fruits (Casado-Vela *et al*., 2006), rice yellow mottle virus infection in rice (Brizard *et al*., 2006), salt stress in tobacco apoplast (Dani *et al*., 2005), and the response to boron deficiency (Alves *et al*., 2006) have been studied recently using proteomic techniques.

Most of the changes observed for protein expression at the subcellular level resulting from PPV infection were related with photosynthesis and carbohydrate metabolism (see Tables 5, 6). Both transketolase and G6PDH are enzymes from the OPPP that play an important role in protection from oxidative stress (Mao-Feng *et al*., 2006). In the early response to PPV, the OPPP appeared to be

Table 3. *Effects of PPV on antioxidant enzymes in soluble fractions and chloroplasts from pea leaves in the initiation phase of infection (3 dpi, early response)*

Data represent the means ±SE from at least three repetitions. Differences from control values are significant at $P < 0.05$ (a), $P < 0.01$ (b), or $P < 0.001$ (c), according to Duncan's multiple range test. nd, Not detectable. *p*HMB-sensitive APX, *p*HMB-insensitive APX, MDHAR, dehydroascorbate reductase (DHAR), GR, and GPX are expressed as nmol min^{-1} mg^{-1} protein, GST, POX, and G6PDH are expressed as μmol min^{-1} mg^{-1} protein Catalase is expressed as mmol min^{-1} mg^{-1} protein and SOD as U mg^{-1} protein.

Enzymatic activity	Soluble fraction		Chloroplasts	
	Control	PPV-inoculated	Control	PPV-inoculated
*p*HMB-sensitive APX	575±56	356±2 a	71±6	33±1.43 b
*p*HMB-insensitive APX	nd	nd	nd	nd
MDHAR	71.7±14.7	67.7±7.3	10.8±0.3	13.2±1.0
DHAR	20.6±3.6	23.5±5.3	14.4±2.1	10.1±1.2
GR	34.6±4.3	38.8±5.1	13.2±1.7	12.1±1.6
GST	9.8±0.9	11.6±0.6	nd	nd
GPOX	nd	nd	38.9±1.9	32.6±0.5
POX	180±1	258±7 c	9.6±1.1	6.5±0.9 b
SOD	51.7±1.3	44.3±3.6	20.4±1.3	16.4±0.5
G6PDH	24.3±1.0	24.9±2.8	2.62±0.04	3.42±0.13 b
Catalase	82.6±3.8	79.9±4.3	nd	nd

Table 4. *Effects of PPV infection on antioxidant enzymes in soluble fractions and chloroplasts from pea leaves in the elaboration phase (15 dpi, disease development)*

Data represent the means ±SE from at least three repetitions. Differences from control values are significant at $P < 0.05$ (a), $P < 0.01$ (b), or $P < 0.001$ (c), according to Duncan's multiple range test. nd, Not detectable. *p*HMB-sensitive APX, *p*HMB-insensitive APX, MDHAR, DHAR, GR, and GPX are expressed as nmol min^{-1} mg^{-1} protein, GST, POX, and G6PDH are expressed as μmol min^{-1} mg^{-1} protein. Catalase is expressed as mmol min^{-1} mg^{-1} protein and SOD as U mg^{-1} protein.

Enzymatic activity	Soluble fraction		Chloroplasts	
	Control	PPV-inoculated	Control	PPV-inoculated
*p*HMB-sensitive APX	269±6	309±9 a	44.0±1.9	38.8±3.8
*p*HMB-insensitive APX	13.5±0.4	23.8±1.5 b	nd	nd
MDHAR	44.4±2.2	50.3±7.0	9.6±0.9	12.9±0.5 a
DHAR	11.4±2.0	11.1±1.9	4.3±0.4	4.2±1.1
GR	26.6±2.5	33.3±3.5	16.1±0.2	9.9±1.8 c
GST	10.6±0.8	7.9±0.4 a	nd	nd
GPOX	nd	nd	74.3±2.8	57.5±4.4 a
POX	73.3±1.1	142.6±5 c	6.5±0.7	6.1±0.3
SOD	12.9±0.9	12.4±2.1	8.8±0.4	5.7±0.4 b
G6PDH	21.9±0.5	18.1±0.6	1.2±0.2	1.6±0.3
Catalase	58.1±3.1	38.4±4.7 a	nd	nd

increased in chloroplasts but not in the soluble fraction, since an increase in G6PDH activity took place only in chloroplasts (Table 3) and, in addition, a decrease in transketolase was detected in soluble fractions in the 2D electrophoresis gels (Table 5). Interestingly, at a longer time (15 dpi), transketolase increased in the soluble fraction (Table 6). The OPPP, besides its important function in NADPH production, also supplies ribose-5-phosphate for the synthesis of ribonucleotides, which can be demanded for virus replication in the cytosol.

The fact that PPV CP was observed by 2D gel electrophoresis only in soluble fractions from PPV-infected plants agrees with the current knowledge that potyviruses replicate and accumulate in the cytoplasm, although there are some published results that found some association of these viruses with chloroplasts (Jiménez *et al*., 2006). This result correlates with the microscopy observations, which showed the presence of GFP and/or PPV in the cytosol of the infected cells (Figs 4, 5). It is not surprising that PPV CP was not detected in the 3 dpi sample, given the low level of virus accumulation at this time, as revealed by the ELISA and RT-PCR analyses.

In chloroplasts, a decrease in polypeptides related with photosynthesis occurred. Already in the initial phase of infection, a decrease in polypeptides showing homology with Rubisco and the OEE protein/complex was observed. The OEE protein/complex has been implicated in photosynthetic oxygen evolution and is associated with the PSII complex, the site of the oxygen evolution in all higher plants and algae (Mayfield *et al*., 1987). In the phase of

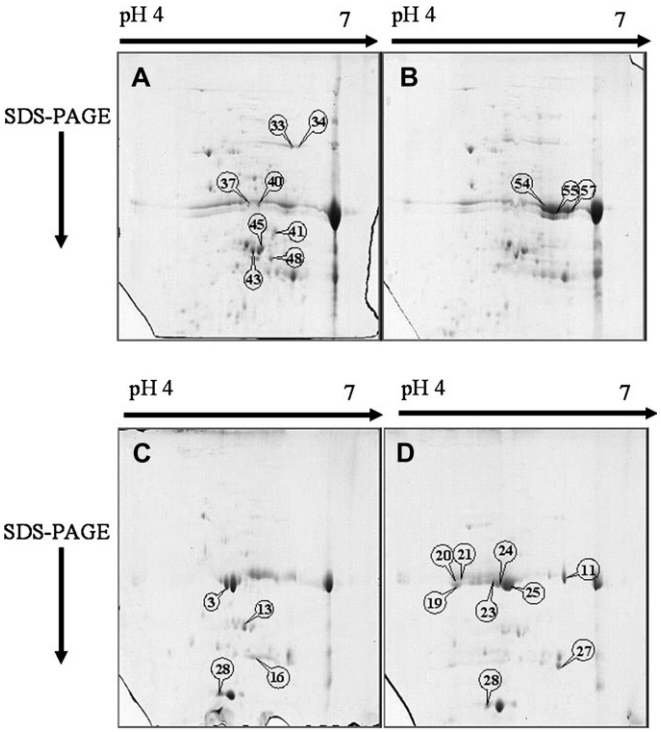

Fig. 8. Reference 2D electrophoretic patterns of soluble and chloroplast fractions from control and PPV-infected pea plants in the initial phase of infection (3 dpi): (A) soluble fraction from control leaves; (B) soluble fraction from inoculated leaves; (C) chloroplast from control leaves; (D) chloroplast from inoculated leaves.

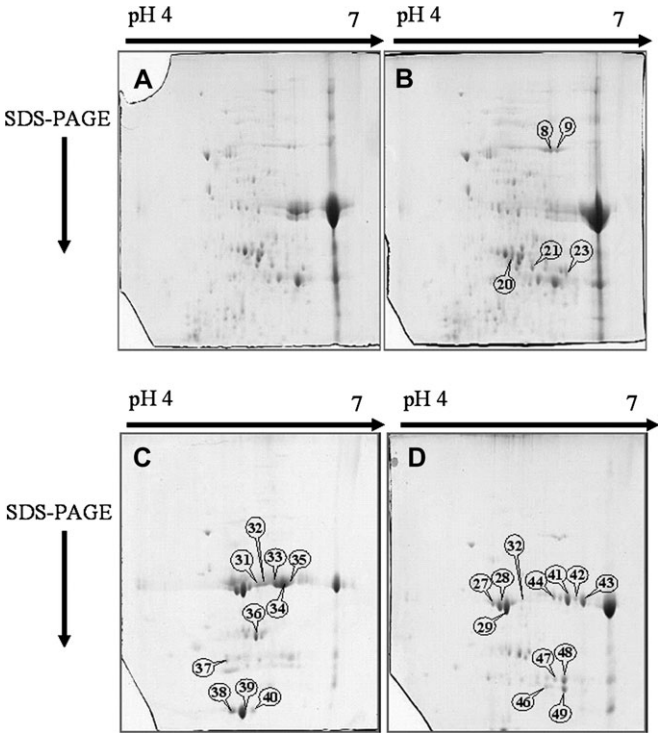

Fig. 9. Reference 2D electrophoretic patterns of soluble and chloroplast fractions from control and PPV-infected pea plants in the phase of disease development (15 dpi): (A) soluble fraction from control leaves; (B) soluble fraction from inoculated leaves; (C) chloroplast from control leaves; (D) chloroplast from inoculated leaves.

disease development, besides the decreases in Rubisco and OEE proteins, a decline in a polypeptide showing homology with the PSII stability/assembly factor also occurred. This protein regulates selectively the biogenesis of PSII and it is essential for the assembly of the reaction centre of PSII (Plücken *et al*., 2002).

It seems that PSII is one of the targets affected by PPV. Different studies revealed that plant viruses produce alterations in the photosynthetic parameters of their host, essentially at the PSII level (Van Kooten *et al*., 1990; Rahoutei *et al*., 2000), although the mechanism of action of the viral infection against PSII remains unclear (Balachandran *et al*., 1997; Rahoutei *et al*., 2000). In CMV-infected tobacco plants, the observed inhibition of PSII activity was associated with a decrease in the amount of the OEE polypeptides (Takahashi and Ehara, 1992), and similar results were obtained in *N. benthamiana* plants infected with different strains of pepper mild mottle virus and paprika mild mottle virus (Rahoutei *et al*., 2000; Perez-Bueno *et al*., 2004). Several authors demonstrated that viral infection can induce in its host a decreased amount of proteins and mRNAs coding for different Calvin cycle enzymes, as well as for the OEE proteins (Rahoutei *et al*., 2000; Perez-Bueno *et al*., 2004). Recent data have shown that damage to OEE activity in virus-infected plants results in a higher viral accumulation in the infected plants (Perez-Bueno *et al*., 2004). In the present study, it seems that, at 15 dpi PPV, effects on photosynthesis were mediated by reductions in the NPQ parameter, the amount of Rubisco, and several polypeptides associated with PSII—three polypeptides with homology with OEE and the PSII stability/assembly factor. The decrease in Rubisco can disturb CO_2 fixation and, accordingly, reduced starch accumulation. In this sense, a correlation between decreases in starch content and Rubisco activity has been described previously in soybean (Scarponi *et al*., 1996).

The PPV effects on photosynthesis during the early phase of infection seem to be also mediated by a reduction in the amount of Rubisco and OEE polypeptides. In addition, at this stage, the decrease in APX observed in chloroplastic fractions could also suggest disruption in the water–water cycle. When this cycle is disrupted by environmental conditions, CO_2 assimilation is lowered and PSI complex can be inhibited (Asada, 1999). In this case, the photosynthetic components would be over-reduced and this would be reflected in the fluorescence parameters, but at this stage no change in these parameters was observed. However, it is reported that the accumulation of H_2O_2 in chloroplasts can lower CO_2 assimilation (Asada, 1999). Moreover, the decrease in Rubisco observed in both infection stages, as mentioned above,

Table 5. *Effect of PPV infection on protein expression in the chloroplasts and soluble fractions from pea plants in the initial phase of infection (3 dpi, early response)*

Spots 27, 33, 34, 40, 41, 43, 45, and 48 were identified by ion trap analysis. All the others were identified by peptide fingerprinting.

Spot no.	Masscot score	pI theor.	MW theor. (Da)	Identification	Variation in expression
Chloroplast					
3, 16	90–228	4.96–5.29	47293–55214	ATP synthase β subunit	Decrease
19, 23, 24, 25	90–296	4.96–5.19	47293–53778	ATP synthase β subunit	Induced
11, 20, 21	150–240	5.47	55031	ATP synthase α chain	Increase
27	590	5.60	41410	ATP synthase γ chain	Increase
13	171	5.54	48186	Rubisco	Decrease
28	153	8.32	49426	Oxygen-evolving enhancer protein	Decrease
Soluble fraction					
37	98	5.19	52124	ATP synthase beta subunit	Decrease
33,34	168–244	6.00	81475	Transketolase	Decrease
40	60		57355	GTP-bindin protein	Decrease
40	10		60281	Leucine aminopeptidase	Decrease
41	190		50555	1-Deoxy-D-xylulose 5-phosphate reductoisomerase	Decrease
43	110		39026	Phosphoribulokinase	Decrease
43	110		93891	Elongation factor 2	Decrease
43	110	6.30	45345	Succinyl CoA ligase/synthetase	Decrease
43, 45	210	8.48	50177	Phosphoglycerate kinase	Decrease
45	210		50177	Chloroplastic precursor Phosphoglycerate kinase	Decrease
43, 48	70–170	8.20	48054	Rubisco activase	Decrease
54, 55, 57	91–342	6.1–6.23	51691–52356	Rubisco	Increase

Table 6. *Effect of PPV infection on protein expression in the chloroplasts and soluble fractions from pea plants in the elaboration phase (15 dpi, disease development)*

All the spots were identified by peptide fingerprinting.

Spot no.	Masscot score	pI theor.	MW theor. (Da)	Identification	Variation in expression
Chloroplast					
27, 28, 29, 32	266–495	4.91–5.22	50887–53383	ATP synthase β subunit	Increase
41, 42, 43, 4 4	207–256	5.47	55031	ATP synthase α chain	Increase
46,49	74–147	8.49	62242	ATP synthase γ chain	Increase
31, 33, 34, 35, 36	209–396	5.54–6.60	48186–51983	Rubisco	Decrease
38, 39, 40	197–323	8.32	49426	Oxygen-evolving enhancer protein	Decrease
37	93		63787	Photosystem II stability factor	Decrease
47, 48	70–74		56669	Aldolase	Increase
Soluble fraction					
8, 9	119–124	6.00	80087	Transketolase	Increase
20	142	5.54	48186	Rubisco	Increase
23	159	5.56	35333	Coat protein	Induced
21	91	5.93	31474	Cytosolic glutamine synthetase	Increase

can result in a diminished CO_2 fixation, which can produce a decrease in the levels of NADPH, the major acceptor of electrons in PSI. Depletion of $NADP^+$ accelerates the reduction of O_2 to $O_2^{\cdot-}$, which is immediately converted to H_2O_2 by SOD (Asada, 1999). So, in both infection phases, the increase in chloroplastic H_2O_2 in PPV-infected plants could be due to this mechanism, which can be influenced also by the reduction of chloroplastic APX and POX activities at 3 dpi and the decrease in the NPQ parameter and GPX activity at 15 dpi. Furthermore, the production of H_2O_2 in chloroplasts may, potentially, inhibit the synthesis of nuclear-encoded proteins because of its ready permeation of membranes (Asada, 1999).

Results indicate that an alteration in the chloroplastic metabolism is produced during the early response to PPV infection favouring the accumulation of ROS in this cell organelle. This oxidative stress is more pronounced during the development of the disease judging from the increase in oxidative stress parameters as well as the imbalance in the antioxidative systems, mainly at the chloroplastic level. According to the proteomic studies, PPV infection affects mainly the photosynthetic metabolism, even during the initiation phase of infection. It seems that PPV has an effect on PSII, directly or indirectly, which could disturb the photosynthetic electron chain that can induce an increase in ROS generation, suggesting that chloroplasts can be a source of oxidative stress during both the

initiation (3 dpi) and the elaboration (15 dpi) phases of viral disease development.

Acknowledgements

This work was supported by the projects 05571/PI/07 (Fundación Séneca, Agencia de Ciencia y Tecnología de la Región de Murcia) and 23BIO2005-04-6444 (Comunidad Autónoma de la Región de Murcia). MJCM thanks the Spanish Ministry of Science and Education for her FPI research fellowship. Authors also thank Mr Jose Ramón Rodriguez for his technical assistance.

References

Alamillo JM, Sáenz P, García JA. 2006. Salicylic acid-mediated and RNA-silencing defense mechanisms cooperate in the restriction of systemic spread of plum pox virus in tobacco. *The Plant Journal* **48,** 217–227.

Alves M, Francisco R, Martins I, Ricardo CPP. 2006. Analysis of *Lupinus albus* leaf apoplastic proteins in response to boron deficiency. *Plant and Soil* **279,** 1–11.

Asada K. 1999. The water–water cycle in chloroplasts: scavenging of active oxygen and dissipation of excess photons. *Annual Review of Plant Physiology and Plant Molecular Biology* **50,** 601–639.

Balachandran S, Hurry VM, Kelley SE, Osmond CB, Robinsos SA, Rohozinski J, Seaton GGR, Sims DA. 1997. Concepts of plant biotic stress: some insights into the stress physiology of virus-infected plants. *Physiologia Plantarum* **100,** 203–213.

Baginsky S, Gruissem W. 2004. Chloroplast proteomic: potentials and challenges. *Journal of Experimental Botany* **55,** 1213–1220.

Bellicampi D, Dipierro N, Salvi G, Cervone F, De Lorenzo G. 2000. Extracellular H_2O_2 induced by oligogalacturonides is not involved in the inhibition of the auxin-regulated roIB gene expression in tobacco leaf explants. *Plant Physiology* **122,** 1379–1385.

Brizard J, Carapito C, Delalande F, Van Dorsselaer A, Brugidou C. 2006. Proteome analysis of plant-virus interactome: comprehensive data for virus multiplication inside their hosts. *Molecular and Cellular Proteomics* **5,** 2279–2297.

Campo S, Carrascal M, Coca M, Abián J, San Segundo B. 2004. The defense response of germinating maize embryos against fungal infection: a proteomic approach. *Proteomics* **4,** 383–396.

Casado-Vela J, Sellés S, Bru Martinez R. 2006. Proteomic analysis of tobacco mosaic virus-infected tomato (*Lycopersicon esculentum* M.) fruits and detection of viral coat protein. *Proteomics* **6,** S196–S206.

Clarke SF, Guy PL, Burritt DJ, Jameson PE. 2002. Changes in the activities of antioxidant enzymes in response to virus infection and hormone treatment. *Physiologia Plantarum* **114,** 157–164.

Dani V, Simon WJ, Duranti M, Croy RRD. 2005. Changes in the tobacco leaf apoplast proteome in response to salt stress. *Proteomics* **5,** 737–745.

del Río LA, Pastori GM, Palma JM, Sandalio LM, Sevilla F, Corpas FJ, Jiménez A, López-Huertas E, Hernández JA. 1998. The activated oxygen role of peroxisomes in senescence. *Plant Physiology* **116,** 1195–1200.

Díaz-Vivancos P, Rubio M, Mesonero V, Periago PM, Ros Barceló A, Martínez-Gómez P, Hernández JA. 2006. The apoplastic antioxidant system in *Prunus*: response to plum pox virus. *Journal of Experimental Botany* **57,** 3813–3824.

Habing WH, Jakoby WB. 1981. Assays for differentiation of glutathione *S*-transferases. *Methods in Enzymology* **77,** 398–405.

Hernández JA, Diaz-Vivancos P, Rubio M, Olmos E, Ros-Barceló A, Martínez-Gómez P. 2006. Long-term PPV infection produces an oxidative stress in a susceptible apricot cultivar but not in a resistant cultivar. *Physiologia Plantarum* **126,** 140–152.

Hernández JA, Ferrer MA, Jiménez A, Ros-Barceló A, Sevilla F. 2001*a*. Antioxidant systems and $O_2^{\cdot-}/H_2O_2$ production in the apoplast of *Pisum sativum* L. leaves: its relation with NaCl-induced necrotic lesions in minor veins. *Plant Physiology* **127,** 817–831.

Hernández JA, Jiménez A, Mullineaux PM, Sevilla F. 2000. Tolerance of pea (*Pisum sativum* L.) to long-term salt stress is associated with induction of antioxidant defenses. *Plant, Cell and Environment* **23,** 853–862.

Hernández JA, Olmos E, Corpas FJ, Sevilla F, del Río LA. 1995. Salt-induced oxidative stress in chloroplast of pea plants. *Plant Science* **105,** 151–167.

Hernández JA, Rubio M, Olmos E, Ros-Barceló A, Martínez-Gómez P. 2004. Oxidative stress induced by long-term Plum Pox virus infection in peach (*Prunus persica* L. cv. GF305). *Physiologia Plantarum* **122,** 486–495.

Hernández JA, Talavera JM, Martínez-Gómez P, Dicenta F, Sevilla F. 2001*b*. Response of antioxidative enzymes to plum pox virus in two apricot cultivars. *Physiologia Plantarum* **111,** 313–321.

Jiménez I, López L, Alamillo JM, Valli A, García JA. 2006. Identification of a plum pox virus CI-interacting protein from chloroplast that has a negative effect in virus infection. *Molecular Plant–Microbe Interactions* **19,** 350–358.

Kölber M. 2001. Workshop on Plum pox. *Acta Horticulturae* **550,** 249–255.

Lansac M, Eyquard JP, Salvador B, García JA, Le Gall O, Decroocq V, Schurdi-Levraud Escalettes V. 2005. Application of GFP-tagged Plum pox virus to study Prunus-PPV interactions at the whole plant and cellular levels. *Journal of Virological Methods* **129,** 125–133.

Mao-Feng C, Peng-Cheng W, Qi-Jun C, Rui A, Jia C Shuhua Y, Xue-Chen W. 2006. NADK3, a novel cytoplasmic source of NADPH, is required under conditions of oxidative stress and modulates abscisic acid responses in *Arabidopsis*. *The Plant Journal* **47,** 665–674.

Martínez-Cordero MA, Martinez V, Rubio F. 2005. High-affinity K^+ uptake in pepper plants. *Journal of Experimental Botany* **56,** 1553–1562.

Martínez-Gómez P, Dicenta F. 2000. Evaluation of resistance of apricot cultivars to a Spanish isolate of plum pox potyvirus (PPV). *Plant Breeding* **119,** 179–181.

Martínez-Gómez P, Dicenta F. 2001. Distribution of coat protein and nucleic acid of *Plum pox virus* (PPV) in seedlings of peach rootstock GF305 and apricot cv. Real Fino. *Phytopathologia Mediterranea* **40,** 157–164.

Mayfield SP, Rahire M, Frank G, Zuber H, Rochaix JD. 1987. Expression of the nuclear gene encoding oxygen-evolving enhancer protein 2 is required for high levels of photosynthetic oxygen evolution in *Chlamydomonas reinhardtii*. *Proceedings of the National Academy of Sciences, USA* **84,** 749–753.

Morales MA, Olmos E, Torrecillas A, Sanchez-Blanco MJ, Alarcon JJ. 2001. Differences in water relations, leaf ion accumulation and excretion rates between cultivated and wild species of *Limonium* sp. grown in conditions of saline stress. *Flora* **196,** 345–352.

Morvan G, Chastelliere M. 1980. An evaluation of herbaceous host of sharka *Plum pox virus*. *Acta Phytopatologica of the Academy of Science of Hungary* **15,** 297–302.

Németh M. 1986. *Virus mycoplasma and rickettsia diseases of fruit trees*. Dordrecht: Martinus Nijhoff Publishers.

Overbaugh JM, Fall R. 1985. Characterization of a selenium-independent glutathione peroxidase from *Euglena gracilis*. *Plant Physiology* **77,** 437–442.

Perez-Bueno ML, Rahoutei J, Sajnani C, García-Luque I, Barón M. 2004. Proteomic analysis of the oxygen evolving complex of photosystem II under biotic stress: studies on *Nicotiana benthamiana* infected with tobamoviruses. *Proteomic* **4,** 418–425.

Plücken H, Müller B, Grohmann D, Westhoff P, Eichacker LA. 2002. The HCF136 protein is essential for assembly of the photosystem II reaction center in *Arabidopsis thaliana*. *FEBS Letters* **532,** 85–90.

Rahoutei J, García-Luque I, Barón M. 2000. Inhibition of photosynthesis by viral infection: effect on PSII structure and function. *Physiologia Plantarum* **110,** 286–292.

Riedel D, Lesemann DE, Maiss E. 1998. Ultrastructural localization of nonstructural and coat proteins of 19 potyviruses using antisera to bacterially expressed proteins of plum pox potyvirus. *Archives of Virology* **143,** 2133–2158.

Riedle-Bauer M. 2000. Role of reactive oxygen species and antioxidant enzymes in systemic virus infections of plants. *Journal of Phytopathology* **148,** 297–302.

Scarponi L, Martinetti L, Alla MMN. 1996. Growth response and changes in starch formation as a result of imazethapyr treatment of soybean (*Glycine max* L.). *Journal of Agricultural and Food Chemistry* **44,** 1572–1577.

Takahashi H, Ehara Y. 1992. Changes in the activity and the polypeptide composition of the oxygen-evolving complex in photosystem II of tobacco leaves infected with cucumber mosaic virus strain Y. *Molecular Plant–Microbe Interactions* **1,** 243–249.

Van Kooten O, Meurs C, Van Loon LC. 1990. Photosynthetic electron transport in tobacco leaves infected with tobacco mosaic virus. *Physiologia Plantarum* **80,** 446–452.

Van Oosten HJ. 1971. Further information about the herbaceous host range of sharka (Plum pox) virus. *Annals of Phytopathology* **2,** 195–201.

Visedo G, Fernández-Piqueras J, García JA. 1990. Isozyme profiles associated with the hypersensitive response of *Chenopodium foetidum* to plum pox virus infection. *Physiologia Plantarum* **78,** 218–224.

Visedo G, Fernández-Piqueras J, García JA. 1991. Peroxidase isozyme analysis of factors involved in development of symptoms in *Nicotiana clevelandii* infected by plum pox virus. *Physiologia Plantarum* **83,** 165–169.

Yi SY, Yu SH, Choi D. 1999. Molecular cloning of a catalase cDNA from *Nicotiana glutinosa* L. and its repression by tobacco mosaic virus. *Molecules and Cells* **9,** 320–325.